Modeling of Light-Driven Bending Vibration of a Liquid Crystal Elastomer Beam

Kai Li
Department of Civil Engineering,
Anhui Jianzhu University,
Hefei, Anhui 230601, China
e-mail: kli@ahjzu.edu.cn

Shengqiang Cai[1]
Department of Mechanical and
Aerospace Engineering,
University of California, San Diego,
La Jolla, CA 92093
e-mail: s3cai@ucsd.edu

In this paper, we study light-driven bending vibration of a liquid crystal elastomer (LCE) beam. Inhomogeneous and time-dependent number fraction of photochromic liquid crystal molecules in cis *state in an LCE beam is considered in our model. Using mode superposition method, we obtain semi-analytic form of light-driven bending vibration of the LCE beam. Our results show that periodic vibration or a statically deformed state can be induced by a static light source in the LCE beam, which depends on the light intensity and position of the light source. We also demonstrate that the amplitude of the bending vibration of the LCE beam can be regulated by tuning light intensity, damping factor of the beam, and thermal relaxation time from* cis *to* trans *state, while the frequency of the vibration in the beam mainly depends on the thermal relaxation time. The method developed in the paper can be important for designing light-driven motion structures and photomechanical energy conversion systems.* [DOI: 10.1115/1.4032073]

1 Introduction

A combination of liquid crystal and polymer network can form a new material—LCE. The special molecular combination makes LCE have many unique properties such as soft or semisoft elasticity [1–4] and multiresponsiveness [5–9], which have led to myriad applications ranging from artificial muscle [7,10] to stretchable optical devices [11–14].

Liquid crystal molecules can rotate in response to various external stimuli such as electric field, temperature variation, magnetic field, and optical field. Because of the direct coupling between the rotation of liquid crystal molecules and the deformation of LCEs, these stimuli can also induce large deformation in LCEs. In particular, some photochromic liquid crystal molecules such as azobenzenes can transform from straight *trans* configuration to bent *cis* configuration by absorbing UV light. As a result, an LCE, containing azobenzenes, can deform under UV light radiation, because the variation of molecular configuration of azobenzenes can change the order degree of liquid crystal molecules, and thus induce strain in LCEs [15–18]. Different from many other external stimuli, one can control light source remotely and precisely focus light on different regions of a material. Therefore, light-actuated materials or structures make various complex photomechanical sensors and actuators possible. Compared to recently intensively developed light-sensitive gels [19], light-sensitive LCEs can respond to light much faster (typically within a second) [20,21].

Because the light absorption in an LCE is usually inhomogeneous and time-dependent, in experiments, dynamic bending of LCE beams or plates can be often observed [22]. For example, it has been shown in experiments that an LCE beam can vibrate steadily without decay for long time with a proper light exposure as shown in Fig. 1 [22]. The system has been proposed to develop to solar energy harvesting devices [23]. Many other dynamic deformation modes in LCE structures under the action of light have also been reported in various experiments [24–26].

Although many theoretical models have been developed to study static or quasi-static deformation of LCE structures, according to our knowledge, no study has been conducted to investigate the dynamics of LCE structures with considering their inertia effects. In the paper, motivated by the recent experiments on the light-driven bending vibration of LCE beams [22–29], we take account of the inertial effect and damping of an LCE beam under static light illumination, and investigate the dynamics of light-driven bending vibration of the beam.

2 Model and Formulation

To model the experiments of light-induced bending vibration of an LCE beam [22–29], we first formulate the dynamics of an LCE cantilever beam exposed to a static light source as sketched in Fig. 1. In the initial state, the LCE beam is flat and its top surface is exposed to the light. Because the LCE tends to contract with absorbing photons, the superficial layer of the top surface of the beam contracts and bends the beam upward. Once the free end of the beam moves upward more than w_0 as shown in Fig. 1, the bottom surface of the beam is exposed to the light while the top surface becomes backlighted. As a result, the superficial layer of the bottom surface of the beam begins to contract and the beam tends to bend downward. As a consequence, the LCE beam can vibrate continuously driven by a static light source.

In the model, the thickness of the LCE cantilever is h and its length is l. We assume that the width of the beam is much larger than its thickness so the beam can be modeled by a plate in plane-strain condition. The dynamics of the deflection of the LCE beam $w(x,t)$ can be governed by

$$\rho_A \frac{\partial^2 w(x,t)}{\partial t^2} + \alpha \frac{\partial w(x,t)}{\partial t} + B \frac{\partial^4 w(x,t)}{\partial x^4} = -\frac{\partial^2 M(x,t)}{\partial x^2} \quad (1)$$

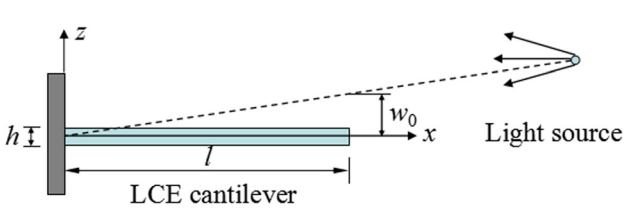

Fig. 1 Schematic model of an LCE cantilever beam with length *l* and thickness *h* exposed to a static light source. The bending stiffness of the beam is $B = Eh^3/12(1-\nu^2)$ with modulus *E* and Poisson's ratio ν, and the mass density of the beam is ρ. The damping factor is α. In the model, the light source is assumed to be far away from the LCE beam.

[1]Corresponding author.

Contributed by the Applied Mechanics Division of ASME for publication in the Journal of Applied Mechanics. Manuscript received September 8, 2015; final manuscript received November 18, 2015; published online December 14, 2015. Editor: Yonggang Huang.

where $\rho_A = \rho h$ with mass density of the LCE beam ρ, α is the damping factor, $B = Eh^3/12(1-\nu^2)$ is the bending stiffness of the LCE beam with modulus E and Poisson's ratio ν, and $M(x,t)$ is the light-induced bending moment.

When the surface of the beam is exposed to light, the light intensity decays exponentially with the penetration depth [30], i.e.,

$$I(z) = I_0 \exp\left(-\frac{|z-z_0|}{d_0}\right) \tag{2}$$

where I_0 is the light intensity on the surface, d_0 is the penetration depth which is typically less than 0.1 mm [31], and z_0 is the vertical coordinate of exposed surface. When the surface of the beam is backlighted, the light intensity $I(z)$ is zero.

To simplify the problem, we assume that the light source is far away from the LCE beam. In addition, we adopt linear plate theory as shown in Eq. (1) by assuming that the slope of the beam is small during the vibration. As a consequence, the incident angle of the light on the surface of the beam does not vary significantly with time and space. Therefore, it is reasonable to assume that the light illumination on either top or bottom surface of the LCE beam is approximately homogeneous and the penetration depth d_0 is also a constant during the beam vibration.

The number fraction of the bent *cis* isomers $\phi(z,t)$ in an LCE depends on thermal excitation from *trans* to *cis*, thermally driven relaxation from *cis* to *trans*, and light-driven isomerization. Thermal excitation from *trans* to *cis* is often negligible relative to the light-driven excitation [32,33]. Therefore, evolution of the number fraction of *cis* isomers $\phi(z,t)$ can be usually described by the governing equation [32–34]

$$\frac{\partial \phi}{\partial t} = \eta_0 I(1-\phi) - T_0^{-1}\phi \tag{3}$$

where T_0 is the thermal relaxation time of the *cis* to *trans* state and η_0 is a light-adsorption constant.

With an initial condition, the solution to Eq. (3) is

$$\phi = \frac{\eta_0 T_0 I}{\eta_0 T_0 I + 1} + \left(\phi_0 - \frac{\eta_0 T_0 I}{\eta_0 T_0 I + 1}\right)\exp\left[-\frac{t}{T_0}(\eta_0 T_0 I + 1)\right] \tag{4}$$

where ϕ_0 is the *cis* number fraction of the photochromic molecules at $t = 0$. For simplicity, we assume $T_0\eta_0 I \ll 1$, which is consistent with most experimental conditions [32,33]. As a consequence, the number fraction of *cis* can be approximately written as

$$\phi(z,t) = \eta_0 T_0 I + (\phi_0 - \eta_0 T_0 I)\exp\left(-\frac{t}{T_0}\right) \tag{5}$$

When the light is off, light intensity $I(z)$ in Eq. (5) is zero. It is noted that the *cis* number fraction ϕ in the LCE beam is both inhomogeneous and time-dependent.

When the initial *cis* number fraction is zero, from Eq. (5), we can easily prove that $\phi(z,t)$ is always linearly proportional to $I(z)$. Consequently, $\phi(x,t)$ can be simply written in the form

$$\phi(z,t) = \begin{cases} \phi_0^+(t)\exp\left(-\dfrac{h/2-z}{d_0}\right) & \text{for} \quad 0 \le z \le h/2 \\ \phi_0^-(t)\exp\left(-\dfrac{h/2+z}{d_0}\right) & \text{for} \quad -h/2 \le z \le 0 \end{cases} \tag{6}$$

where $\phi_0^+(t)$ and $\phi_0^-(t)$ are the number fraction of *cis* isomers on the upper surface and bottom surface of the LCE beam at time t, respectively. In Eq. (6), we also implicitly assume that the light penetration depth d_0 is much smaller than the thickness of the beam.

As shown in Fig. 1, we define w_0 based on the geometric setup of the point light source and the cantilever beam. The slope of the beam during the bending vibration is assumed to be small. Therefore, to a good approximation, we assume that the upper surface of the beam is homogeneously exposed to the light illumination when the deflection of the free end of the beam w_{end} is less than w_0, and the lower surface is homogeneously exposed to light illumination when the deflection of the free end of the beam w_{end} is larger than w_0.

We assume that the light-driven contraction strain $\varepsilon_0(z,t)$ is linearly proportional to the small *cis* number fraction $\phi(z,t)$, so the light-driven contraction in the beam is

$$\varepsilon_0(z,t) = -C_0\phi(z,t) \tag{7}$$

where C_0 is the contraction coefficient. Therefore, the light-induced momentum in the beam can be calculated by the integration

$$M(x,t) = \frac{E}{1-\nu}\int_{-h/2}^{h/2} \varepsilon_0(z,t) z dz \tag{8}$$

The moment in Eq. (8) is independent of x, so we have $\partial M(x,t)/\partial x = -M(x,t)\delta(x-l)$ in Eq. (1).

With Eqs. (6)–(8), Eq. (1) can be rewritten and nondimensionalized as

$$\frac{\partial^2 \overline{w}(\bar{x},\bar{t})}{\partial \bar{t}^2} + \bar{\alpha}\frac{\partial \overline{w}(\bar{x},\bar{t})}{\partial \bar{t}} + \frac{\partial^4 \overline{w}(\bar{x},\bar{t})}{\partial \bar{x}^4} = \frac{\partial \overline{M}(\bar{x},\bar{t})}{\partial \bar{x}} \tag{9}$$

where $\overline{w} = w/l$, $\bar{x} = x/l$, $\bar{t} = t/l^2\sqrt{\rho_A/B}$, $\bar{\alpha} = \alpha l^2/\sqrt{\rho_A B}$ and

$$\overline{M}(\bar{x},\bar{t}) = -m(\bar{t})\delta(\bar{x}-1) \tag{10}$$

with

$$m(\bar{t}) = \overline{T}_0\overline{I}_0[\overline{\phi}_0^+(\bar{t}) - \overline{\phi}_0^-(\bar{t})] \tag{11}$$

where dimensionless thermal relaxation time of *cis* to *trans* state is defined as: $\overline{T}_0 = T_0/l^2\sqrt{\rho_A/B}$, dimensionless light intensity is defined as: $\overline{I}_0 = 12I_0\eta_0 C_0 l^2\sqrt{\rho_A/B}(1+\nu)\bar{d}_0^2[\bar{h}/2\bar{d}_0 - 1 + \exp(-\bar{h}/2\bar{d}_0)]/\bar{h}^3$, dimensionless light penetration depth is defined as: $\bar{d}_0 = d_0/l$, and dimensionless thickness of the beam is defined as: $\bar{h} = h/l$, $\overline{\phi}_0^+ = \phi_0^+/T_0\eta_0 I_0$, and $\overline{\phi}_0^- = \phi_0^-/T_0\eta_0 I_0$. We further nondimensionalize the deflection of the end of the beam and the light source position as $\overline{w}_{\text{end}} = w_{\text{end}}/l$ and $\overline{w}_0 = w_0/l$, respectively.

The initial conditions for the LCE beam are

$$\overline{w}(\bar{x},\bar{t}=0) = 0 \tag{12}$$

and

$$\frac{\partial \overline{w}(\bar{x},\bar{t}=0)}{\partial \bar{t}} = 0 \tag{13}$$

Following mode superposition method in Ref. [35], the solution of the partial differential equation (9) can be written as

$$\overline{w}(\bar{x},\bar{t}) = \sum_{j=1}^{\infty} q_j(\bar{t})Y_j(\bar{x}) \tag{14}$$

where $Y_j(\bar{x})$ is the canonical principal vibration mode of cantilever

$$Y_j(\bar{x}) = \cosh(\beta_j\bar{x}) - \cos(\beta_j\bar{x}) - \frac{\sinh(\beta_j) - \sin(\beta_j)}{\cosh(\beta_j) + \cos(\beta_j)}\left[\sinh(\beta_j\bar{x}) - \sin(\beta_j\bar{x})\right] \tag{15}$$

with β_j the jth root of the eigen-equation $\cos(\beta_i)\cosh(\beta_i) = -1$: $\beta_1 = 1.875$, $\beta_2 = 4.694$, $\beta_3 = 7.855$, $\beta_4 = 10.996$, etc.

Inserting Eq. (14) into Eq. (9) leads to

$$\frac{d^2 q_j(\bar{t})}{d\bar{t}^2} + 2\zeta_j \omega_j \frac{dq_j(\bar{t})}{d\bar{t}} + \omega_j^2 q_j(\bar{t}) = P_j(\bar{t}) \tag{16}$$

where $\omega_j = \beta_j^2$, $\zeta_j = \bar{\alpha}/2\omega_j$, and $P_j(\bar{t}) = Y_j'(1)m(\bar{t})$.

The solution of ordinary differential equation (16), with initial conditions (12) and (13), can be given by Duhamel integration

$$q_j(\bar{t}) = \frac{1}{\omega_{dj}} \int_0^{\bar{t}} Y_j'(1) m(\tau) \exp\left[-\zeta_j \omega_j (\bar{t} - \tau)\right] \sin\left[\omega_{dj}(\bar{t} - \tau)\right] d\tau, \tag{17}$$

where $\omega_{dj} = \omega_j \sqrt{1 - \zeta_j^2}$ is the natural frequency of jth vibration mode of the beam.

To calculate the bending vibration of the LCE beam under the action of light illumination, we first need to calculate $q_j(\bar{t})$ using the integration (17) for different time. In Eq. (17), $m(\tau)$ can be determined from Eq. (11), in which $\overline{\phi}_0^+(\bar{t})$ and $\overline{\phi}_0^-(\bar{t})$ can be obtained from the deformation history of the beam and the population dynamics in Eq. (5). Once $q_j(\bar{t})$ is computed, by inserting $q_j(\bar{t})$ and $Y_j(\bar{x})$ into Eq. (14), the deflection $w(\bar{x}, \bar{t})$ can be finally obtained.

3 Results and Discussion

The formulation in Sec. 2 shows that the bending vibration of LCE beam depends on light intensity, light source position, damping factor, and thermal relaxation time. We first estimate the typical range of the dimensionless parameters in our model. A typical time scale of thermal relaxation time of *cis* to *trans* state is $T_0 \approx 10^{-1}$s [20,21] and the light penetration depth is typically $d \approx 10^{-5}$m [31]. Elastic modulus of the LCE is estimated to be $E \approx 1$MPa. The experiments on the light-driven vibration of LCE beams enable us to estimate geometric parameters of the beam [25,27]: $h \approx 10^{-4}$m and $l \approx 10^{-2}$m. The damping coefficient is set to be $\alpha \approx 1$ kg s^{-1} m^{-2}. Therefore, the dimensionless characteristic relaxation time is $\overline{T}_0 = T_0/l^2\sqrt{\rho_A/B} \approx 1$, and the dimensionless damping factor is $\bar{\alpha} = \alpha l^2/\sqrt{\rho_A B} \approx 1$. The dimensionless light intensity is assumed to be around 0.1, namely, $\bar{I}_0 \approx 0.1$. Based on Eqs. (5) and (7) and other dimensionless parameters, we can estimate that the light-induced eigenstrain on the exposed surface of the beam is around 0.1%, which can be easily realized in a photosensitive LCE with small light absorption [32]. In the following, we will use the results we have obtained to discuss the effects of all the above parameters of the system. A qualitative comparison between our calculations and experimental observations will be also discussed at the end of this section.

Figure 2 illustrates the influence of light intensity on the light-driven vibration of the LCE beam. In the calculation, we fix thermal relaxation time of the *cis* to *trans* state $\overline{T}_0 = 0.2$, damping factor $\bar{\alpha} = 1$, and light source position $\overline{w}_0 = 0.02$. Figure 2 shows that two different states of the LCE beam can be driven by the light exposure. Figure 2(*a*) demonstrates that when the light intensity is small, e.g., $\bar{I}_0 = 0.025$, the LCE beam can quickly evolve to a new deformed equilibrium state after a few cycles of vibration. When the light intensity increases, e.g., $\bar{I}_0 = 0.05$, steady and periodic vibration of the LCE beam can be induced by the light as shown in Fig. 2(*b*). The results indicate that the light intensity needs to be high enough to trigger steady vibration of the beam. When the light intensity exceeds a critical value, the deflection of the free end of the beam bent by light can be larger than $\overline{w}_0$. Consequently, the top surface (also the bottom surface) of the beam will be exposed to light and backlighted periodically, and the LCE beam can vibrate.

Figure 2(*c*) plots temporal history of the deflection of the free end of the LCE beam with light intensity $\bar{I}_0 = 0.075$. By comparing Figs. 2(*b*) and 2(*c*), we can see that with increasing light intensity $\bar{I}_0$ from 0.05 to 0.075, amplitude of the vibration of the free end of the LCE beam increases from 0.02 to 0.03. The result is consistent with that all the equations in Sec. 2 linearly depend on the light intensity $\bar{I}_0$. Figures 2(*b*) and 2(*c*) also show that beam vibration frequency is not affected by the light intensity.

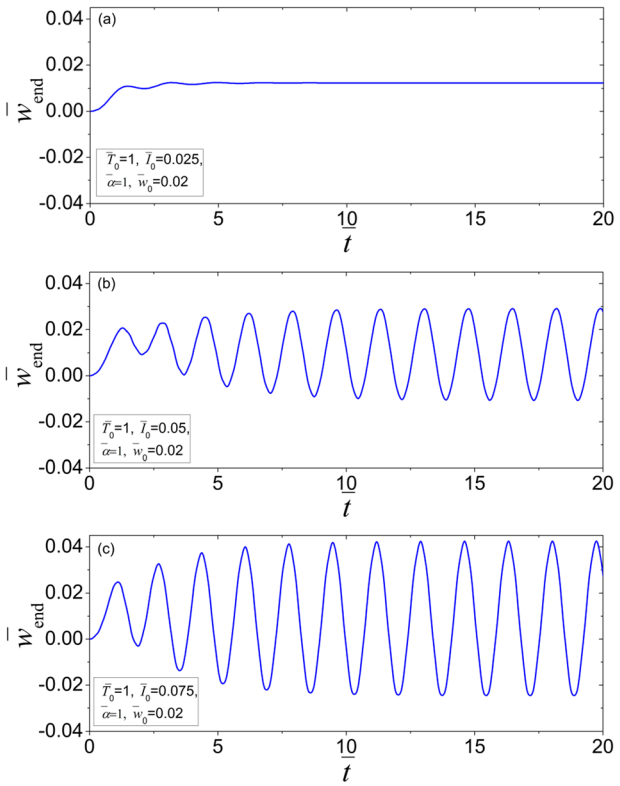

Fig. 2 Two states of the LCE beam can be induced by light, depending on the light intensity $\bar{I}_0$: (*a*) a statically deformed state ($\bar{I}_0 = 0.025$) and (*b*) periodic vibration state ($\bar{I}_0 = 0.05$). (*c*) The amplitude of light-driven vibration increases with increasing light intensity ($\bar{I}_0 = 0.075$). In the calculation, we fix the parameters: thermal relaxation time of the *cis* to *trans* state $\overline{T}_0 = 1$, damping factor $\bar{\alpha} = 1$, and light source position $\overline{w}_0 = 0.02$.

Figure 3 illustrates the influence of light source position on the vibration of the LCE beam. In the calculation, we fix the thermal relaxation time of the *cis* to *trans* state $\overline{T}_0 = 0.2$, light intensity $\bar{I}_0 = 0.25$, and damping factor $\bar{\alpha} = 1$. For large $\overline{w}_0$, the LCE beam evolves to a new equilibrium state (Fig. 3(*a*)). For smaller $\overline{w}_0$, periodic vibration of the LCE beam can be driven, as shown in Figs. 3(*b*) and 3(*c*). These results are similar to that in Figs. 2(*a*) and 2(*b*). For a fixed light intensity, the light source position needs to be low enough to trigger steady vibration of the beam. Figures 2 and 3 indicate that a combination of light intensity and light source position determines whether steady vibration can be triggered by a static light source in the LCE beam.

As shown in Figs. 3(*b*) and 3(*c*), once the LCE beam can vibrate steadily, both the amplitude and frequency of the vibration are not strongly affected by the light source position. However, with moving light source upward from $\overline{w}_0 = 0.001$ (Fig. 3(*c*)) to $\overline{w}_0 = 0.01$ (Fig. 3(*b*)), the vibration center of the free end of the beam also moves upward. This is because when the free end of the beam deflects passing w_0, the top surface and bottom surface of the beam switch between exposed state and backlighted state periodically.

Figure 4 illustrates the influence of damping factor on the light-driven vibration of the LCE beam. In the calculation, we fix the thermal relaxation time $\overline{T}_0 = 0.2$, light intensity $\bar{I}_0 = 0.1$, and

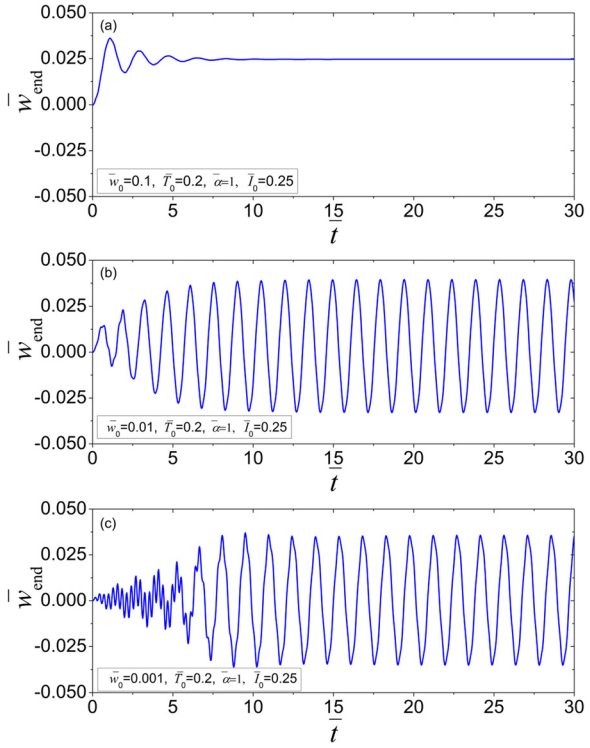

Fig. 3 Influence of light source position on the light-driven vibration of the LCE beam. The positions of the light source are: (*a*) $\overline{w}_0 = 0.1$, (*b*) $\overline{w}_0 = 0.01$, and (*c*) $\overline{w}_0 = 0.001$. Light source position can also determine whether the light can induce the beam vibration. In the calculation, we fix the parameters: thermal relaxation time of the *cis* to *trans* state $\overline{T}_0 = 0.2$, damping factor $\overline{\alpha} = 1$, and light intensity $\overline{I}_0 = 0.25$.

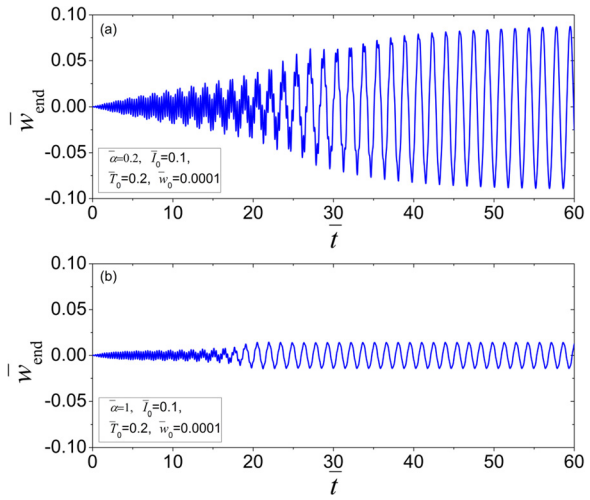

Fig. 4 Influence of damping factor $\overline{\alpha}$ on the light-driven vibration of the LCE beam. In the calculation, we choose (*a*) $\overline{\alpha} = 0.2$ and (*b*) $\overline{\alpha} = 1$. The amplitude decreases with increasing damping factor. In the calculation, we fix the parameters: light intensity $\overline{I}_0 = 0.1$, thermal relaxation time of the *cis* to *trans* state $\overline{T}_0 = 0.2$, and light source position $\overline{w}_0 = 0.0001$.

light source position $\overline{w}_0 = 0.0001$. The results show that the damping factor can greatly influence the amplitude of the vibration. With increasing the damping factor from $\overline{\alpha} = 0.2$ (Fig. 4(*a*)) to $\overline{\alpha} = 1$ (Fig. 4(*b*)), the amplitude of vibration decreases significantly. This can be simply understood by the energy conversion of the system. In the process of the beam vibration, optical energy absorbed by the LCE beam compensates the dissipated energy due to the damping. The dissipated energy depends on the magnitude of both damping factor and vibration. Therefore, with constant light source, to keep the dissipated energy unchanged, the vibration amplitude has to decrease when the damping factor increases. Figures 2 and 4 imply that the amplitude of the light-driven vibration in the LCE beam can be regulated by tuning the light intensity and the magnitude of damping factor.

Figure 4 also shows that the magnitude of damping factor affects the vibration frequency negligibly. In the system, the damping process is assumed to have no effect on light-driven isomerization and thermally driven relaxation. However, the damping factor can influence the natural frequency of the beam vibration as $\omega_{dj} = \beta_j^2\sqrt{1-\overline{\alpha}^2/4\beta_j^4}$. For small damping factor $\overline{\alpha}$, the natural frequency ω_{dj} changes negligibly with the variation of damping factor $\overline{\alpha}$.

Figures 2–4 show that the frequency of light-driven oscillation is almost independent of light intensity, light source position, and damping factor. The discussion below reveals that the LCE beam vibration frequency is mainly determined by the thermal relaxation time of the *cis* to *trans* state.

In Fig. 5, we plot the deflection of the free end of the LCE beam with the thermal relaxation time of the *cis* to *trans* state: $\overline{T}_0 = 0.3$ and 0.1, respectively. In the calculation, we fix light intensity $\overline{I}_0 = 0.2$, damping factor $\overline{\alpha} = 1$, and light source position $\overline{w}_0 = 0.0001$. Figures 5(*a*) and 5(*b*) show that the frequencies of the two light-driven vibrations are significantly different. The period of the beam vibration for thermal relaxation time $\overline{T}_0 = 0.3$ is about 1.8 (Fig. 5(*a*)), which is the intrinsic period of the first-order vibration mode of the beam. However, the period of the beam vibration for thermal relaxation time $\overline{T}_0 = 0.1$ (Fig. 5(*b*)) is equal to the intrinsic period of the second-order vibration of the LCE beam. The results indicate that when the thermal relaxation time is large, the light can trigger first-order vibration mode with low frequency (Fig. 5(*a*)), which is the case for all the previous experiments [22,25,27]. When the thermal relaxation time is small enough, the light can induce high-order vibration mode of the LCE beam as shown in Fig. 5(*b*).

Bending vibration of the beam is caused by periodic light-driven isomerization, which is the result of the coupling between light-driven isomerization and vibration of the beam. Therefore,

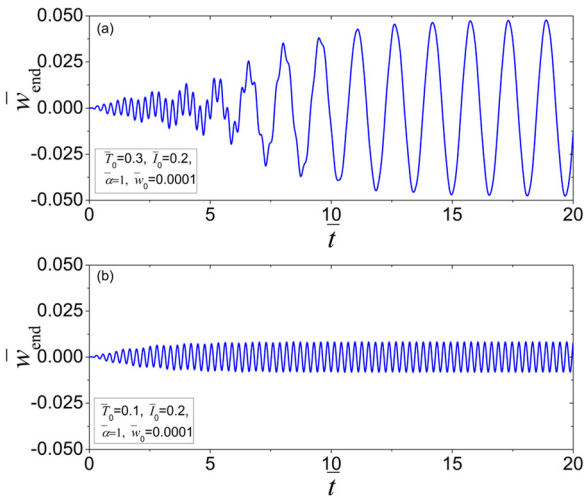

Fig. 5 Influence of thermal relaxation time of the *cis* to *trans* state $\overline{T}_0$ on the light-driven vibration in the LCE beam. (*a*) We set thermal relaxation time $\overline{T}_0 = 0.3$, first-order vibration mode is induced in the LCE beam. (*b*) We set thermal relaxation time $\overline{T}_0 = 0.1$, second-order vibration mode is induced in the beam with smaller amplitude. The other parameters used in the calculations are light intensity $\overline{I}_0 = 0.2$, damping factor $\overline{\alpha} = 1$, and light source position $\overline{w}_0 = 0.0001$.

for large thermal relaxation time of the *cis* to *trans* state T_0, first-order vibration mode in the beam with low frequency can be induced. For small thermal relaxation time of the *cis* to *trans* state T_0, high-order vibration mode in the beam with higher frequency can be triggered. This is further demonstrated by the calculated vibration mode shown in Fig. 6.

In Fig. 6, we plot the snapshots of vibrations of the LCE beam for Figs. 5(*a*) and 5(*b*). Figure 6(*a*) shows that the beam vibration mainly consists of the first-order vibration mode of the LCE beam, while Fig. 6(*b*) shows that the beam vibration mainly consists of the second-order vibration mode of the LCE beam. The result is consistent with the discussion above. Figures 5 and 6 imply that different vibration mode of the LCE beam can be driven by the light with different thermal relaxation time.

We would like to point out that our calculations of the second or higher vibration mode in the LCE beam may not be accurate, because we simply assume that the whole surface (top or bottom) is always exposed to the light homogeneously, which is not true for the beam with second or higher order vibration mode. Certain modifications need to be made in the modeling to study higher order vibration modes in the LCE beam driven by light.

Figures 5 and 6 also show that the amplitudes of the vibration also depend on the thermal relaxation time of the *cis* to *trans* state $\overline{T}_0$. With decreasing thermal relaxation time $\overline{T}_0$, the amplitude of the vibration decreases. From the population dynamics law of Eq. (5), the *cis* number fraction decreases with decreasing thermal relaxation time. Therefore, for shorter thermal relaxation time, the light-driven equivalent momentum is smaller. A combination of Figs. 2, 4, and 5 shows that the amplitude of light-driven vibration can be controlled by tuning the light intensity, damping factor, and thermal relaxation time of the *cis* to *trans* state.

Although our modeling is mainly motivated by several similar experimental setups, detailed and quantitative measurements of the vibration of an LCE beam triggered by light illumination are not available in the literature. Therefore, a direct comparison between our predictions and experimental measurements is not possible at this moment. Instead, we would like to qualitatively link some experimental observations of the light-driven bending vibration of LCE beams to our predictions.

It has been shown in the experiments [25,27] that the power density of the laser beam needs to be high enough to trigger the beam vibration, which is consistent with our predictions as shown in Figs. 2(*a*) and 2(*b*). The experiments have further shown that the vibration amplitude of the LCE beam increases with the increase of power density of the laser beam, but the frequency of the bending vibration of the beam is almost unaffected by the power density of the laser beam. The experimental results also agree with our predictions as shown in Figs. 2(*b*) and 2(*c*). In the experiments, the effects of the air pressure on the bending vibration of an LCE beam have also been examined. It has shown that the increase of air pressure results in the decrease of the vibration amplitude of the beam. However, the frequency of the vibration was almost unaffected by the change of air pressure. As illustrated in Fig. 4, the experimental measurements of the effects of the surrounding air pressure have been also correctly captured by the effect of damping factor α in our model.

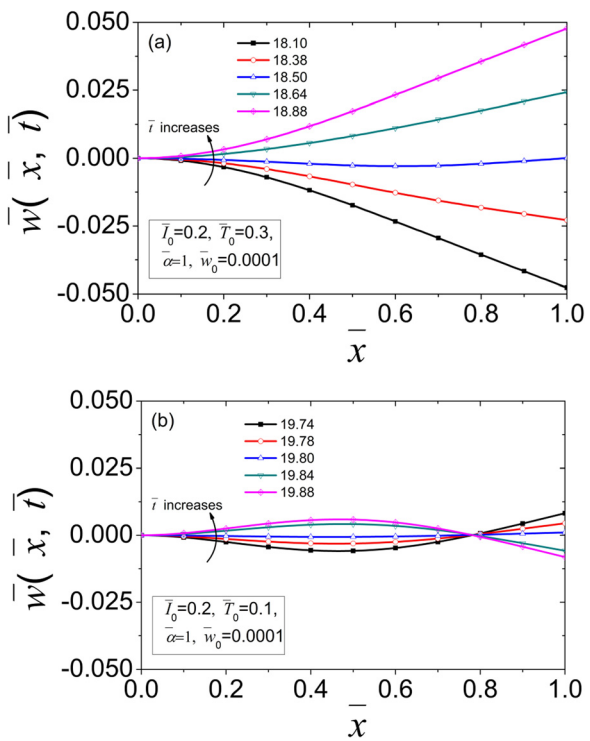

Fig. 6 Snapshots of light-induced bending vibration of the LCE beam, for Figs. 5(*a*) and 5(*b*). (*a*) For thermal relaxation time of the *cis* to *trans* state $\overline{T}_0 = 0.3$, first-order vibration mode in the beam is driven by the light. (*b*) For thermal relaxation time of the *cis* to *trans* state $\overline{T}_0 = 0.1$, second-order vibration mode in the beam is driven by the light.

4 Conclusions

In this paper, we studied light-driven vibration of an LCE beam. The presented model takes account of the inhomogeneous and time-dependent *cis* number fraction in the LCE beam. We obtain semi-analytic form of light-driven vibration of the LCE beam using mode superposition method. Our calculations show that periodic vibration or statically deformed state of the LCE beam can be induced by a constant light source. When light intensity is smaller than a critical value, the LCE beam vibrates with decayed amplitude and finally reaches a statically deformed state. When light intensity is large enough, steady and periodic vibration of the LCE beam can be driven by the light.

The amplitude of the light-driven vibration of the LCE beam can be manipulated by tuning light intensity, damping factor, and thermal relaxation time of the *cis* to *trans* state. With increasing light intensity, or decreasing damping factor, or increasing thermal relaxation time, the vibration amplitude increases. By controlling the light source position, we can change the vibration center of the LCE beam. For different thermal relaxation time, different vibration modes in the beam can be excited by the light. The method developed in the paper can be important for designing light-driven motion structures and photomechanical energy conversion systems.

Acknowledgment

Kai Li acknowledges the supports from Chinese Natural Science Foundation (Grant Nos. 11402001 and 11472005), Anhui Provincial Natural Science Foundation (Grant No. 1408085QA18), and Natural Science Fund of Education Department of Anhui Province (Grant No. KJ2014ZD07). Shengqiang Cai acknowledges the funds from Haythornthwaite Foundation.

References

[1] Dey, S., Agra-Kooijman, D. M., Ren, W., McMullan, P. J., Griffin, A. C., and Kumar, S., 2013, "Soft Elasticity in Main Chain Liquid Crystal Elastomers," Crystals, **3**(2), pp. 363–390.

[2] Biggins, J. S., Warner, M., and Bhattacharya, K., 2012, "Elasticity of Polydomain Liquid Crystal Elastomers," J. Mech. Phys. Solids, **60**(4), pp. 573–590.

[3] Brown, A. W., and Adams, J. M., 2012, "Negative Poisson's Ratio and Semi-soft Elasticity of Smectic-C Liquid-Crystal Elastomers," Phys. Rev. E, **85**(1), p. 011703.

[4] Adams, J. M., and Warner, M., 2005, "Soft Elasticity in Smectic Elastomers," Phys. Rev. E, **72**(1), p. 011703.

[5] Corbett, D., and Warner, M., 2009, "Changing Liquid Crystal Elastomer Ordering With Light—A Route to Opto-Mechanically Responsive Materials," Liq. Cryst., **36**(10–11), pp. 1263–1280.

[6] Dawson, N. J., Kuzyk, M. G., Neal, J., Luchette, P., and Palffy-Muhoray, P., 2011, "Modeling the Mechanisms of the Photomechanical Response of a Nematic Liquid Crystal Elastomer," J. Opt. Soc. Am. B, **28**(9), pp. 2134–2141.
[7] Wermter, H., and Finkelmann, H., 2001, "Liquid Crystalline Elastomers as Artificial Muscles," e-Polymers, **1**(1), pp. 111–123.
[8] Petsch, S., Rix, R., Khatri, B., Schuhladen, S., Müller, P., Zentel, R., and Zappe, H., 2015, "Smart Artificial Muscle Actuators: Liquid Crystal Elastomers With Integrated Temperature Feedback," Sensor. Actuat. A, **231**, pp. 44–51.
[9] Xing, H. H., Li, J., Guo, J. B., and Wei, J., 2015, "Bio-Inspired Thermal-Responsive Inverse Opal Films With Dual Structural Colors Based on Liquid Crystal Elastomer," J. Mater. Chem. C, **3**(17), pp. 4424–4430.
[10] Li, M. H., and Keller, P., 2006, "Artificial Muscles Based on Liquid Crystal Elastomers," Philos. Trans. R. Soc., A, **364**(1847), pp. 2763–2777.
[11] Schmidtke, J., Kniesel, S., and Finkelmann, H., 2005, "Probing the Photonic Properties of a Cholesteric Elastomer Under Biaxial Stress," Macromolecules, **38**(4), pp. 1357–1363.
[12] Schmidtke, J., Stille, W., Finkelmann, H., and Kim, S. T., 2002, "Laser Emission in a Dye Doped Cholesteric Polymer Network," Adv. Mater., **14**(10), pp. 746–749.
[13] Dawson, N. J., Kuzyk, M. G., Neal, J., Luchette, P., and Palffy-Muhoray, P., 2011, "Cascading of Liquid Crystal Elastomer Photomechanical Optical Devices," Opt. Commun., **284**(4), pp. 991–993.
[14] Shilov, S. V., Skupin, H., Kremer, F., Skarp, K., Stein, P., and Finkelmann, H., 1998, "Segmental Motion of Ferroelectric Liquid Crystal Polymer and Elastomer During Electro-Optical Switching," Proc. SPIE, **3318**, pp. 62–67.
[15] Krishnan, D., and Johnson, H. T., 2014, "Light-Induced Deformation in a Liquid Crystal Elastomer Photonic Crystal," J. Mech. Phys. Solids, **62**, pp. 48–56.
[16] Li, M. E., Lv, S., and Zhou, J. X., 2014, "Photo-Thermo-Mechanically Actuated Bending and Snapping Kinetics of Liquid Crystal Elastomer Cantilever," Smart Mater. Struct., **23**(12), p. 125012.
[17] Dunn, M. L., and Maute, K., 2009, "Photomechanics of Blanket and Patterned Liquid Crystal Elastomer Films," Mech. Mater., **41**(10), pp. 1083–1089.
[18] Dunn, M. L., 2007, "Photomechanics of Mono- and Polydomain Liquid Crystal Elastomer Films," J. Appl. Phys., **102**(1), p. 013506.
[19] Hauser, A. W., Evans, A. A., Na, J. H., and Hayward, R. C., 2015, "Photothermally Reprogrammable Buckling of Nanocomposite Gel Sheets," Angew. Chem., Int. Ed., **54**(18), pp. 5434–5437.
[20] Camacho-Lopez, M., Finkelmann, H., Palffy-Muhoray, P., and Shelley, M., 2004, "Fast Liquid Crystal Elastomer Swims Into the Dark," Nat. Mater., **3**(5), pp. 307–310.
[21] Nagele, T., Hoche, R., Zinth, W., and Wachtveitl, J., 1997, "Femtosecond Photoisomerization of *Cis*-Azobenzene," Chem. Phys. Lett., **272**(5–6), pp. 489–495.
[22] Garcia-Amoros, J., Nonell, S., and Velasco, D., 2011, "Photo-Driven Optical Oscillators in the kHz Range Based on Push–Pull Hydroxyazopyridines," Chem. Commun., **47**(13), pp. 4022–4024.
[23] Hiscock, T., Warner, M., and Palffy-Muhoray, P., 2011, "Solar to Electrical Conversion Via Liquid Crystal Elastomers," J. Appl. Phys., **109**(10), p. 104506.
[24] Torras, N., Zinoviev, K. E., Marshall, J. E., Terentjev, E. M., and Esteve, J., 2011, "Bending Kinetics of a Photo-Actuating Nematic Elastomer Cantilever," Appl. Phys. Lett., **99**(25), p. 254102.
[25] Serak, S., Tabiryan, N., Vergara, R., White, T. J., Vaia, R. A., and Bunning, T. J., 2010, "Liquid Crystalline Polymer Cantilever Oscillators Fueled by Light," Soft Matter, **6**(4), pp. 779–783.
[26] Shankar, M. R., Smith, M. L., Tondiglia, V. P., Lee, K. M., McConney, M. E., Wang, D. H., Tan, L., and White, T. J., 2013, "Contactless, Photoinitiated Snap-Through in Azobenzene-Functionalized Polymers," Proc. Natl. Acad. Sci. U.S.A., **110**(47), pp. 18792–18797.
[27] White, T. J., Tabiryan, N. V., Serak, S. V., Hrozhyk, U. A., Tondiqlia, V. P., Koerner, H., Vaia, R. A., and Bunning, T. J., 2008, "A High Frequency Photodriven Polymer Oscillator," Soft Matter, **4**(9), pp. 1796–1798.
[28] Lee, K. M., Smith, M. L., Koerner, H., Tabiryan, N., Vaia, R. A., Bunning, T. J., and White, T. J., 2011, "Photodriven, Flexural–Torsional Oscillation of Glassy Azobenzene Liquid Crystal Polymer Networks," Adv. Funct. Mater., **21**(15), pp. 2913–2918.
[29] Shimamura, A., Priimagi, A., Mamiya, J. I., Kinoshita, M., Ikeda, T., and Shishido, A., 2011, "Photoinduced Bending Upon Pulsed Irradiation in Azobenzene-Containing Crosslinked Liquid-Crystalline Polymers," J. Nonlinear Opt. Phys., **20**(4), pp. 405–413.
[30] Corbett, D., and Warner, M., 2007, "Linear and Nonlinear Photoinduced Deformations of Cantilevers," Phys. Rev. Lett., **99**(17), p. 174302.
[31] Marshall, J. E., and Terentjev, E. M., 2013, "Photo-Sensitivity of Dye-Doped Liquid Crystal Elastomers," Soft Matter, **9**(35), pp. 8547–8551.
[32] Finkelmann, H., Nishikawa, E., Pereira, G. G., and Warner, M., 2001, "A New Opto-Mechanical Effect in Solids," Phys. Rev. Lett., **87**(1), p. 015501.
[33] Hogan, P. M., Tajbakhsh, A. R., and Terentjev, E. M., 2002, "UV Manipulation of Order and Macroscopic Shape in Nematic Elastomers," Phys. Rev. E, **65**(4), p. 041720.
[34] Jin, L. H., Lin, Y., and Huo, Y. Z., 2011, "A Large Deflection Light-Induced Bending Model for Liquid Crystal Elastomers Under Uniform or Non-Uniform Illumination," Int. J. Solids Struct., **48**(22–23), pp. 3232–3242.
[35] Thomson, W. T., and Dahleh, M. D., 1998, *Theory of Vibration With Applications*, 5th ed., Prentice Hall, Upper Saddle River, NJ.